Journal of Applied Geophysics 73 (2011) 101–110

Contents lists available at ScienceDirect

Journal of Applied Geophysics

journal homepage: www.elsevier.com/locate/jappgeo

Traveltime inversion and error analysis for layered anisotropy

Fan Jiang *, Hua-wei Zhou

Department of Geosciences, Texas Tech University, Lubbock, TX, 79409-1053, United States

ARTICLE INFO

Article history:
Received 16 July 2010
Accepted 2 December 2010
Available online 21 December 2010

Keywords:
Anisotropy
First arrivals
Acquisition geometry
Traveltime tomography
Parameter estimation

ABSTRACT

While tilted transverse isotropy (TTI) is a good approximation of the velocity structure for many dipping and fractured strata, it is still challenging to estimate anisotropic depth models even when the tilted angle is known. With the assumption of weak anisotropy, we present a TTI traveltime inversion approach for models consisting of several thickness-varying layers where the anisotropic parameters are constant for each layer. For each model layer the inversion variables consist of the anisotropic parameters ε and δ, the tilted angle φ of its symmetry axis, layer velocity along the symmetry axis, and thickness variation of the layer. Using this method and synthetic data, we evaluate the effects of errors in some of the model parameters on the inverted values of the other parameters in crosswell and Vertical Seismic Profile (VSP) acquisition geometry. The analyses show that the errors in the layer symmetry axes sensitively affect the inverted values of other parameters, especially δ. However, the impact of errors in δ on the inversion of other parameters is much less than the impact on δ from the errors in other parameters. Hence, a practical strategy is first to invert for the most error-tolerant parameter layer velocity, then progressively invert for ε in crosswell geometry or δ in VSP geometry.

1. Introduction

Seismic anisotropy, the variation of the propagation speed of seismic waves as a function of traveling direction, may be caused by alignments of mineral crystals, fractures, and thin layers of alternative velocities. When sedimentation and tectonic processes produce dip and thickness variations in rock layers, the velocity structures may be approximated as a tilted transverse isotropy, or TTI media. For sedimentary strata with a short depositional history the symmetry axes are assumed to be vertical; and for old strata that have undergone tectonic deformation the symmetry axes tend to be normal to bedding (Hornby et al., 1994; Sayers, 2005). In thrust belts like that in the Canadian foothills (Charles et al., 2008), reservoirs are overlain by thick sequences of dipping sandstone and shale layers which result in a tilted symmetry axes which vary with the layer geometries. The tilted angles of symmetry make it more challenging to estimate the model parameters for TTI media as compared to that for VTI (vertical transverse isotropy) media or for HTI (horizontal transverse isotropy) media.

Explicit estimations of velocity anisotropy are not commonly incorporated into seismic imaging process, largely due to the difficulties in estimating the orientation and magnitude of the anisotropy in depth models. However, the parameter estimation in transversely isotropic media has attracted considerable attention, mostly in time-domain analysis using surface reflection data (Alkhalifah and Tsvankin, 1995). A commonly-used approach is based on non-hyperbolic NMO type analysis. The layer stripping process using the Dix formula has been shown as a feasible tool for time-domain anisotropic analysis (Dewangan and Tsvankin, 2006). For a transversely isotropic model with vertical axis, the P-wave velocity is controlled by the axial velocity V_{p0} and the anisotropic parameters ε and δ (Thomsen, 1986). Alkhalifah and Tsvankin (1995) illustrated that only two parameters, the NMO velocity from a horizontal reflector and the anellipticity coefficient η, can be used for anisotropic analysis if the medium above the reflector is laterally homogeneous. Hence, semblance has been considered as an effective tool to define stacking velocity (Alkhalifah, 1997). The semblance coefficient is defined as the ratio of the output energy over a window of a stack of traces to the input energy in the unstacked traces. Estimating the semblance velocity is based on summing data over hyperbolic trajectories controlled by the trial moveout velocity. Kumar et al. (2008) proposed a common-focus point domain analysis for anisotropic parameter estimation. In this domain, errors in imaging are seen as non-zero differential time shifts, the estimate of anisotropic parameters ε and δ is obtained using least-square solutions of Newton's equation that make the differential time shifts zero.

One of the conclusions that can be drawn from the literature is that building anisotropic velocity model from the surface reflection data in time domain brings ambiguities (Sen and Mukherjee, 2003; Tsvankin and Thomsen, 1994). One reason is that time domain processes are based on layer stripping approach with the Dix formula. It will result in instability due to the accumulation of errors during the procedure.

* Corresponding author. Department of Geosciences, Texas Tech University, Lubbock, TX 79409-1053, United States. Tel.: +1 281 546 2725; fax: +1 806 742 0100.
E-mail address: fan.jiang@ttu.edu (F. Jiang).

0926-9851/$ – see front matter © 2010 Elsevier B.V. All rights reserved.
doi:10.1016/j.jappgeo.2010.12.001

It is still a bottleneck to reconstruct anisotropic models for prestack migration using the time domain analyses. On the other hand, in depth domain, seismic tomography is a promising approach to estimate the distributions of anisotropic parameters (Chapman and Pratt, 1992). Watanabe et al. (1996) presented a seismic traveltime tomography approach to estimate anisotropic slowness and orientation simultaneously in anisotropic heterogeneous media. Kumar et al. (2004) proposed a ray-based method to calculate TTI traveltime that relies on the computations of group velocity from neighboring eight points. Zhou et al. (2008) proposed a nonlinear kinematic inversion method for crosswell seismic tomography in composite transversely isotropic media with known dipping symmetry axes. Charles et al. (2008) evaluated how anisotropic model building strategies affect seismic imaging in the Canadian Foothills by comparing the results of a model-driven approach with a data-driven approach. Some studies showed that fault plane reflection energy that intersects sedimentary reflectors may be helpful to estimate anisotropic parameters (Ball, 1995). However, these studies show that reliable estimates of layered anisotropic parameters in model space are difficult even when the tilted symmetry axes are known. A major challenge is to determine depth variations of velocity interfaces and anisotropy-induced discrepancies together, especially if only first arrivals are available. Simplifications like models with planar interfaces or fixed interface geometries have been implemented to constrain the inversion processes.

In this paper, we devise a traveltime tomography method using TTI models with several thickness-varying layers and assume that the anisotropic parameters are constant for each model layer in the presence of weak anisotropy. The inversion variables for each layer are the two anisotropic parameters ε and δ, the tilted angle φ of the symmetry axis, layer velocity or slowness along the symmetry axis, and the thickness variations of the layer. Considering the varying ability to invert for different model parameters, we search for ways to invert only for some of the variables in such layered TTI models while fixing the other variables using their default values. By applying the layered tomography method to a series of simple synthetic models, we analyze the impacts of errors in some of the model parameters on the sensitivities of the other parameters. Several experiments suggest that in crosswell acquisition geometry, axial velocity and ε should be considered for priority inversion variables. However, in the VSP acquisition geometry, because most raypaths spread around 45°, δ can be considered as priority inversion parameter as well as axial velocity.

2. Layered anisotropic traveltime tomography

In anisotropic media, the expression for the P-wave phase velocity has been obtained by Thomsen (1986) under the weak anisotropy approximation:

$$V_p(\phi) = V_p(0)\left(1 + \delta\, sin^2(\phi)\, cos^2(\phi) + \varepsilon\, sin^4(\phi)\right) \tag{1}$$

where $V_p(\boldsymbol{\phi})$ is phase velocity at incident angle $\boldsymbol{\phi}$, $V_p(0)$ is vertical velocity, ε and δ are anisotropic parameters. The above equation is obtained by extending the exact expression of the phase velocity in a Taylor series in the small parameters ε and δ at fixed $\boldsymbol{\phi}$ (Thomsen, 1986). The group velocity expression, $V_g(\theta)$, is obtained from Thomsen's derivation (Thomsen, 1986):

$$V_g^2(\theta) = V_p^2(\phi) + \left(\frac{dV_p(\phi)}{d\phi}\right)^2 \tag{2}$$

where θ is the ray angle from the source point to the wavefront. Under weak anisotropy approximation, the relationship between ray angle θ and phase angle $\boldsymbol{\phi}$ of P wave is given by Thomsen (1986):

$$tan(\theta) = tan(\phi)\left(1 + 2\delta + 4(\varepsilon-\delta)\, sin^2(\phi)\right). \tag{3}$$

Substituting Eqs. (1) and (2) into (3) retaining only linear terms in the small parameters ε, δ and θ shown on Eq. (4) (Sena, 1991):

$$V_g^{-2}(\theta) = V_g^{-2}(0)\left(1-2\delta\, sin^2(\theta)+2(\delta-\varepsilon)\, sin^4(\theta)\right). \tag{4}$$

By adding a tilted angle φ of symmetry axis into Eq. (4), we can obtain traveltime equation in TTI media:

$$V_g^{-2}(\theta-\varphi) = V_g^{-2}(0)\left(1-2\delta\, sin^2(\theta-\varphi)+2(\delta-\varepsilon)\, sin^4(\theta-\varphi)\right) \tag{5}$$

where $(\theta-\varphi)=\gamma$ is the group angle, or ray angle (Fig. 1). Eq. (5) has three advantages over other traveltime equations: (1) fast traveltime calculation using the group velocity; (2) easy generation of Frechet's kernels for tomographic inversion; (3) providing physical insight into the wave propagation in anisotropic media. To facilitate traveltime inversion, we extended shortest-path ray tracing (Moser, 1991) from isotropic to an anisotropic model by combining with Eq. (5) and obtain linear ray-based traveltime equation:

$$t = len_{ray} * sw_{p0} * \sqrt{1-2\delta\, sin^2(\theta-\varphi)+2(\delta-\varepsilon)\, sin^4(\theta-\varphi)} \tag{6}$$

where t is traveltime and len_{ray} is the distance along the raypath, sw_{p0} is the P-wave slowness along the symmetry axis, or the axial slowness. The ray angle $(\theta-\varphi)$ can be directly measured from two neighboring ray tracing nodes with particular symmetry axis (Fig. 1). By varying arbitrarily tilted angles of symmetry, the shortest-path ray tracing method is adaptive for generating P wave wavefront in TTI media by implementing Eq. (6) (Fig. 2). Fig. 3 shows a comparison of the first arrivals generating by anisotropic shortest-path ray tracing approach and acoustic finite difference waveform modeling (Zhou et al., 2006) in multi-layered TTI models. The first arrivals from ray tracing approach are in good agreement with that from waveform modeling with less computation time.

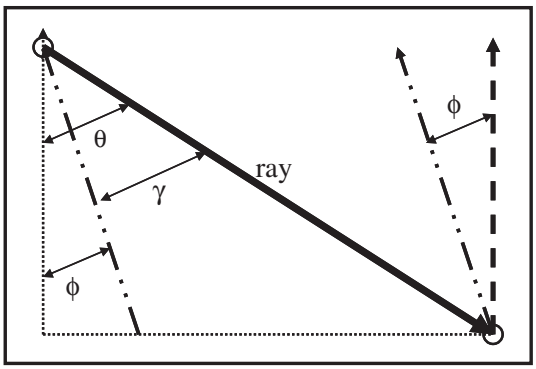

Fig. 1. A sketch to illustrate the TTI model. Variable φ is the tilted angle between vertical axis (dash line) and tilted symmetry axis (long dash dot line), θ is the angle between vertical axis and ray path (solid line), γ is the ray angle, or group angle ($\theta-\varphi$).

Anisotropic traveltime tomography uses traveltimes of seismic waves to constrain anisotropic velocity variations. Cell-based anisotropic tomography inverts for velocity and anisotropic parameters as a function of spatial location (Zhou et al., 2008), the velocity is resolvable where there are a sufficient number of intersecting rays. However, poor ray angle coverage leads to smear artifacts bearing the imprint of the raypaths and poor resolution of anisotropic anomalies (Cerveny, 2001). Therefore, layered tomography was developed to update the geometries of velocity interfaces using residual traveltimes of reflectors (Bishop et al., 1985; Kosloff et al., 1996). Zhou (2006) introduced a deformable layered traveltime tomography that incorporates a priori knowledge of velocity and subsurface geometry information on major stratigraphic units and lithologic boundaries. The traveltime residual for the ith ray in layered tomography (Zhou, 2006) is:

$$\delta t_i = \sum_j^J k\_s_{ij}\delta s_j + \sum_l^L k\_z_{il}\delta z_l, \tag{7}$$

where δs_j is the slowness perturbation of the jth layer, k_s_{ij} is the slowness kernel, δz_l is the interface perturbation at the lth node, and k_z_{il} is the interface kernel. J is the total number of slowness and L is the total number of the interface nodes to be inverted. Introducing anisotropy brings one more term to the traveltime residual:

$$\delta t_i = \sum_j^J k\_s_{ij}\delta s_j + \sum_l^L k\_z_{il}\delta z_l + \sum_g^G k\_\xi_{ig}\delta\xi_g \tag{8}$$

where $\delta\xi_g$ is the perturbation of the gth TTI parameters, such as ε, δ or the titled angle φ, and k_ξ_{ig} is the corresponding kernel. Eq. (8) describes that in anisotropic layered traveltime tomography, the residual traveltime is a compound with axial velocity, layer geometry, anisotropic parameters ε, δ and tilted symmetry axis. The variation in one of those parameters will affect the total residual traveltime. Nonuniqueness between those five parameters becomes unavoidable and there is a need to declare the sensitivity of each parameter on the traveltime to estimate the most error-tolerant parameters.

Take the first derivative of Eq. (6) with respect to different TTI parameters, the analytical expressions for the Frechet kernels can be easily derived. The Frechet kernel for the axial slowness is

$$\frac{\partial t}{\partial\left(sw_{p0}\right)} = len_{ray}{}^{*}\left(1-2\delta\ sin^2\gamma+2(\delta-\varepsilon)\ sin\boldsymbol{\gamma}^4\right)^{1/2}. \tag{9a}$$

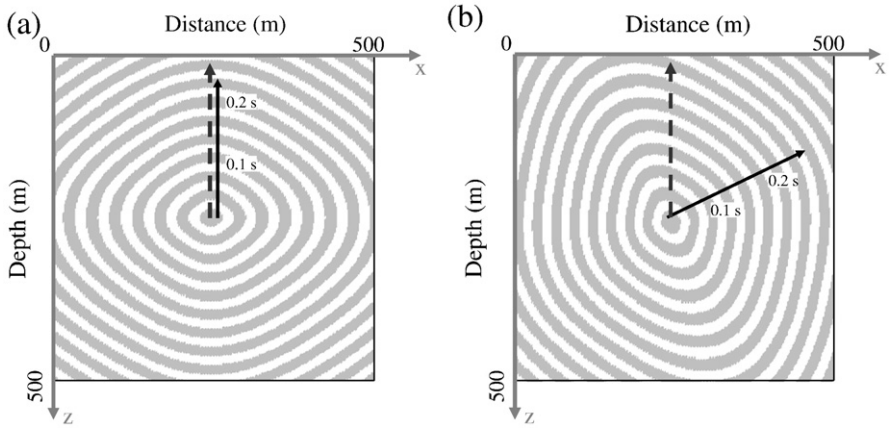

Fig. 2. The P-wave wavefronts in TI media with the different tilted angle φ, generating by TTI ray tracing. (a) $\varphi=0°$ (VTI). (b) $\varphi=-67°$. Here $sw_{p0}=1$ s/km, $\varepsilon=0.18$, $\delta=-0.12$. Dash line presents the vertical axis and solid line represents the direction of the tilted symmetry axis.

(a)

	Vp_0(km/s)	ε	δ	ϕ
Layer1	2.0	0.10	-0.04	20°
Layer2	2.5	0.12	-0.06	30°
Layer3	3.0	0.14	-0.08	40°
Layer4	3.5	0.16	-0.10	50°

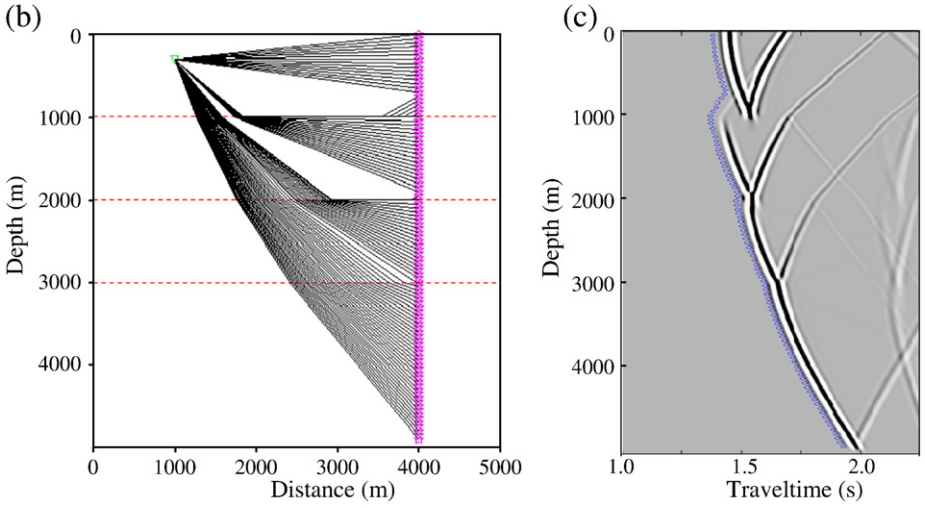

Fig. 3. The comparison between TTI ray tracing and TTI waveform modeling. (a) Anisotropic parameters in each layer. (b) TTI shortest path ray tracing. (c) Common shot gather generated by TTI acoustic wave equation (Zhou et al., 2006). The dotted line indicates the picked first arrival traveltime from (b).

The kernels for the anisotropic parameters ε and δ are

$$\frac{\partial t}{\partial \varepsilon} = \frac{-\left(len_{ray}{}^{*} sw_{p0}{}^{*} \sin^4\gamma\right)}{\sqrt{1-2\delta \sin^2\gamma + 2(\delta-\varepsilon)\sin^4\gamma}}, \tag{9b}$$

$$\frac{\partial t}{\partial \delta} = \frac{len_{ray}{}^{*} sw_{p0}{}^{*}\left(\sin^4\gamma - \sin^2\gamma\right)}{\sqrt{1-2\delta \sin^2\gamma + 2(\delta-\varepsilon)\sin^4\gamma}}. \tag{9c}$$

In deriving the kernel for the tilted angle of the symmetry axis, we take the sine function of the tilted angle φ as the variable to obtain

$$\frac{\partial t}{\partial(\sin(\varphi))} = len_{ray}{}^{*} sw_{p0}{}^{*} \frac{\left[2\delta \sin(\gamma)(\sin(\theta)tg(\varphi) + \cos(\theta)\cos(\varphi)) + 4(\varepsilon-\delta)\sin^3(\gamma)(\sin(\theta)tg(\varphi) + \cos(\theta)\cos(\varphi))\right]}{\sqrt{1-2\delta \sin^2(\gamma) + 2(\delta-\varepsilon)\sin^4(\gamma)}}. \tag{9d}$$

Finally for the interface k_z_{il}, the analytical formulation is not available, except for simple cases (Kosloff et al., 1996; Zhou, 2003). In this paper, the interface kernels are estimated numerically following that in Zhou (2006). The calculated Frechet derivatives can be used for a model parameterization explicitly and directly used in any local search minimization inversion algorithm, such as conjugate gradient (Scales, 1987) or Gauss–Newton (Pratt et al., 1998) to yield the elements of the Jacobian matrix directly for arbitrary model parameterization. Each Frechet kernel presents the rates of change in the observations to perturbations in cell or medium properties, such as Thomsen's anisotropic parameter. Therefore, the Frechet kernels are examined as sensitivity functions of the data to a particular parameter and indicate the sensitivity variations with various surveying configurations (Zhou and Greenhalgh, 2009).

Each of the above kernels depicts the sensitivity of the traveltime to the corresponding inversion variable, hence quantifying the resolvability for the variable. Based on the analytical kernels, the sensitivity of traveltime to key TTI parameters as a function of the ray angles for a specified set of anisotropic parameters is shown in Fig. 4. At the same ray angle, the sensitivity of the traveltime to different TTI parameters can be quite different. For instance, the axial velocity has best sensitivity in all angle range, it can be considered as first priority inversion parameter in any acquisition geometry. The kernel for ε reaches to a high peak around ray angle 90°, meaning that ε is most resolvable using rays along the direction normal to the tilt symmetry axis, which indicates crosswell geometry may be the best acquisition geometry to resolve ε. The kernel for δ reaches to its peak around ray angle 45°, hence it indicates that δ may be resolvable using rays along 45° direction, meaning that δ could be easily recovered in VSP acquisition geometry. The kernel for sine function of tilted angle φ reaches to a broad peak with intermediate magnitude between ray angle 60° and 80°, indicating it has a similar sensitivity trend but less tolerant to

noise in comparison with that for ε. Since the magnitude of the kernel for ε is much greater (more than four times in this case) than that for δ in the range of large ray angles, it is generally much easier to use traveltimes to invert for ε than for δ in crosswell geometry, but the reversed assumption holds true in VSP acquisition geometry. The tilted angle φ shows the average resolvability in both VSP and crosswell geometries, it could be inverted after estimating ε in crosswell geometry or δ in VSP geometry. Though a simple anisotropic model with one set of the parameter values is used to show the sensitivity of the traveltime to the inversion variables here, we may expect a similar trend in the sensitivity for more complicated TTI models as mosaics of the simple model.

3. Error evaluation of TTI inversion using synthetic models

Considering the varying resolvability for different TTI model parameters in traveltime inversion, we want to evaluate the influence of errors in each of the TTI parameters on the inverted results of other parameters. Because in many applications the data coverage may not allow for reliable inversion of all TTI parameters, our evaluation may lead to a practical strategy to invert for the most resolvable TTI parameters in particular acquisition geometry. The evaluation is facilitated by applying the new layered traveltime tomography method to a series of synthetic models. Since the true model is known, the synthetic tests allow us to quantify the relative ability to recover each of the TTI parameters in the presence of errors in other parameters.

To facilitate a meaningful comparison between the inversion errors of the different model parameters, we define a normalized form of the error:

$$\text{Error} = \frac{m^{\text{true}} - m^{\text{pred}}}{m^{\text{range}}} \times 100\% \tag{10}$$

where m^{true} stands for the true or observed value of the parameter such as the value of the true model in a synthetic test, m^{pred} stands for the predicted value from a model, such as the initial reference model, or the inverted value of the parameter. m^{range} stands for the possible range of the parameter in the inversion based on the known understandings (Thomsen, 1986; Tsvankin, 2001). In this study we assign a range of −20% to +20% for both ε and δ, hence the denominator in Eq. (10) is 0.4 for ε and δ. Without loss of generality, in the synthetic models of this study the range for the axial velocity of each layer is from 1 to 4 km/s, and the range of the tilted angle of the symmetry axis is from −50° to +50°. Since Thomsen's parameters are represented by the ratios of velocities and the size of errors for inherent anisotropy scale, the parameter m^{range} is specified to quantify how sensitive each parameter is affected by errors from other parameters. In this study, we use Eq. (10) to quantify errors in the initially referenced model parameters, and we also use the absolute value of Eq. (10) to quantify the impact of errors in each parameter on the inversion results of other parameters.

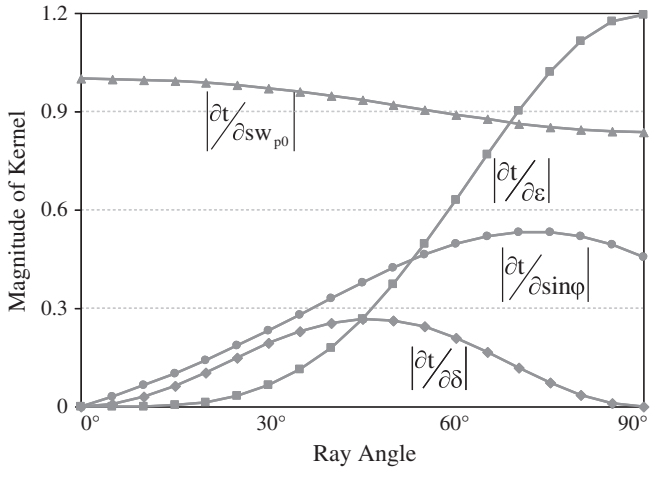

Fig. 4. The sensitivity of traveltime to key TTI parameters as a function of the ray angles. Here, $sw_{p0} = 1$ s/m, $len_{ray} = 1$ m, $\varepsilon = 0.15$ and $\delta = 0.1$ for calculating kernels using Eq. (4)(a)–(d). The kernel of sine function of tilted angle φ is calculated with the assumption of 45° tilted angle.

3.1. 2D block model TTI parameter estimations using first arrivals

We start by the simple case of a 2D TTI layered traveltime tomography in a block model. The simulation is to determine anisotropic properties in a single piece of rock that has a set of pre-defined anisotropic parameters. We use crosswell geometry and a combination of crosswell plus VSP acquisition geometry (Fig. 5) that give different patterns in the raypath coverage. The noise-free data, computed by anisotropic shortest-path ray tracing approach, are used as the observed data to examine how accurately the parameters can be recovered by inverting the axial velocity, anisotropic parameters ε and δ, and the tilted angle φ of the symmetry axis together. The values of the model parameters in the initial reference model differ much from that in the true model. Table 1 lists the values for one of the inversion tests by TTI layered traveltime tomography. In this case all of the inversion parameters are resolved very well because of good ray coverage.

Though δ is one of the significant parameters describing velocity anisotropy (Berryman et al., 1999; Thomsen, 1986), it is questionable that whether errors on δ have a strong influence on other parameters using conventional acquisition geometries. Here we analyze the impact of errors in δ on the inversions of other parameters by TTI layered traveltime tomography. By setting δ to zero value in the true model but using different δ values in the initial reference model, we invert for the axial velocity, ε, and the tilted angle φ together. The error of δ is different between its value in the true model and in the reference model. This error behaves as noise to the inversions of the other model parameters. Tables 2 and 3 show the statistic errors from the tests of TTI layered traveltime tomography using different levels of the noise in δ. Even when the noise in δ reaches to 25%, it caused only 1.1% error in the inverted value for the axial velocity, 0.8% error in the inverted value for ε, and 0.6% error in the inverted value for the tilted angle φ in the case of crosswell acquisition geometry. In the case of crosswell plus VSP recording geometry, the inverted error is reduced to 0.7% in the axial velocity, 0.5% in the ε value, and 0.6% in the tilted angle φ. These results indicate that in crosswell acquisition geometry, the errors in δ may not bring large impact on the inversion results of other parameters in such cases with a wide angle coverage of raypath.

The symmetry axes of the TTI anisotropy may be altered due to thrusting and other deformations. Since we assume an effective symmetry axis for each model layer, additional errors in the symmetry axis may occur. Here we consider the impact of noise in the tilted angle φ of the symmetry axis on the inversion results of other parameters. We assign 10% error in the tilted angle φ and invert for the axial velocity, ε and δ together. Using the crosswell recording geometry, this 10% noise in the tilted angle φ can cause 1.7% error in the inverted axial velocity, 3.8% error in the inverted ε, and 18.3% error in the inverted δ. Using the crosswell plus VSP geometry, due to the improved ray coverage with more raypaths along the 45° angle (for δ) and near-90° angle (for ε), the 10% noise in the tilted angle φ caused only 0.2% error in the inverted axial velocity, 0.8% error in the inverted ε value, and 2.5% error in the inverted δ value. These synthetic tests suggest that, in terms of their priorities for inversion, the axial velocity and ε may not be largely affected by the errors from the tilted angle of symmetry axis or δ, they

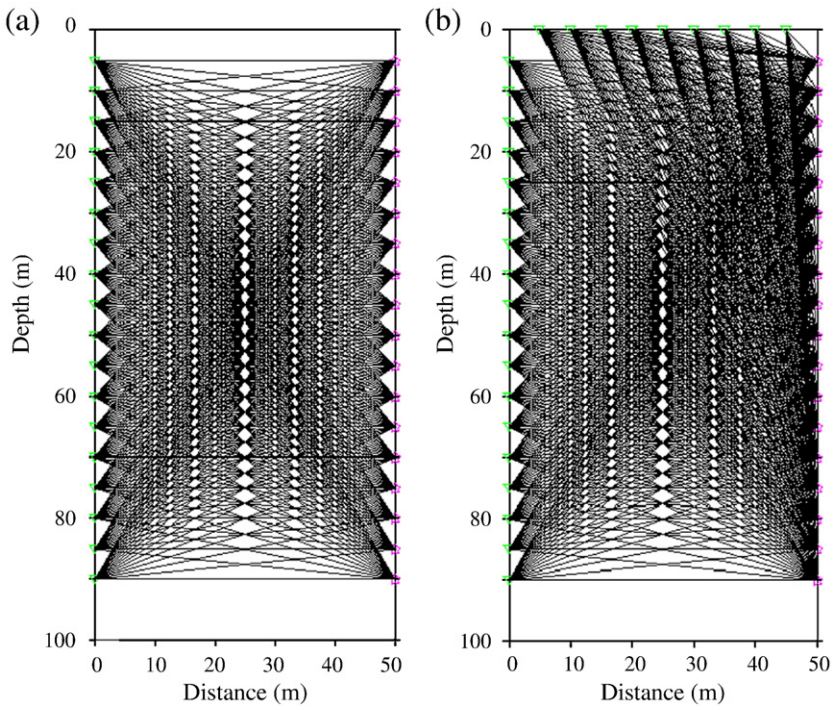

Fig. 5. Two seismic recording geometries and their relative raypaths in a single block model. (a) Crosswell geometry. (b) Crosswell plus VSP geometry. The triangle indicates the source, and the star indicates the receiver.

could be considered as primary parameters to estimate in the crosswell case. After synthetically adding VSP on crosswell geometry, the quality of inverted δ is increased significantly. This indicates that the resolvability of δ is indeed sensitive with the ray angle around 45° and could be recovered properly in the VSP acquisition geometry.

3.2. 2D layered model TTI parameter estimation using crosswell first arrivals

A previous experiment provides preliminary results on the resolvability of different anisotropic parameters in crosswell-dominated acquisition geometry. Crosswell tomography can provide a wide ray angle coverage and check shot velocity, hence estimating layer geometry becomes feasible. We further show a TTI layered traveltime tomography for the interface geometry, ε and the tilted angle φ in a crosswell acquisition geometry (Fig. 6). We experiment two inversions with different δ assumptions to test the robustness of this approach and quantify the influence of δ on other parameters. In inversion I (Fig. 6c), δ is assumed to be a correct value in each layer, however in inversion II (Fig. 6d), δ is assumed to be zero in each layer and is considered as noise in data space.

Both inversions perform twelve iterations and final results show good approximations. Inversion I is well resolved with the average solution errors of 0.58% for ε and 0.45% for tilted angle φ. The average solution errors for inversion II are 1.85% for ε and 2.27% for φ. Those inversions verify that in crosswell acquisition geometry, even without δ information, other TTI parameters still can be recovered properly. Because the difficulty to estimate accurate δ in crosswell geometry, we may treat δ as a constant value from geological information or estimate δ from the moveout analysis.

By adding 5% Gaussian noise of traveltime data, we further invert for layer geometries, ε and tilted angle φ of symmetry axes while parameter δ are fixed during the inversion process. Fig. 7 shows that the TTI layered traveltime tomography still make the geological sense with approximate structure and acceptable anisotropic parameters after twelve iterations when 5% Gaussian noise is added.

3.3. 2D layered model TTI parameter estimation using VSP first arrivals

VSP has been good acquisition geometry to detect anisotropy (Maultzsch et al., 2007; Slawinski et al., 2003). A major challenge is to distinguish the effect of depth variations of velocity interfaces from that caused by anisotropy in the layer velocities, especially if only the first arrivals are used. Simplifications like model with planar interface or fixed interface geometry have been implemented to help constrain the velocity models using VSP first arrivals. Here we first evaluate the inversion for the interface geometry and anisotropic parameters ε and δ using VSP first arrivals (Fig. 8). The values of the true three-layer model are, from the top to bottom layers, the P-wave axial velocities of 2.0, 2.5, 3.0 km/s, and the tilted angles of 10°, −10°, 1° for the symmetry axes in these layers. Assigning tilted angle 1° for bottom

Table 1
Anisotropic parameters in a 2D single block model and solutions using two different recording geometries.

	True model	Initial model	Crosswell solution	Crosswell plus VSP solution
V_{p0} [km/s]	2.0	2.5	2.000	2.000
ε	0.15	0.0	0.150	0.150
δ	0.10	0.0	0.101	0.100
φ [°]	25	0	24.999	25.000

Table 2
Inversion errors using four levels of noise in δ with the crosswell geometry.

δ in the true model	δ in the initial reference model	Given error of δ	Inversion errors of other parameters		
			V_{p0}	ε	φ
0.0	0.10	−25.0%	1.1%	0.8%	0.6%
	0.05	−12.5%	0.5%	0.5%	0.8%
	−0.05	12.5%	0.5%	0.5%	0.2%
	−0.10	25.0%	1.1%	1.0%	0.5%

Table 3
Inversion errors using four levels of noise in δ with the crosswell plus VSP geometry.

δ in the true model	δ in the initial reference model	Given error of δ	Inversion errors of other parameters		
			V_{p0}	ε	φ
0.0	0.10	−25.0%	0.7%	0.5%	0.6%
	0.05	−12.5%	0.3%	0.3%	0.5%
	−0.05	12.5%	0.3%	0.3%	0.6%
	−0.10	25.0%	0.4%	0.5%	0.8%

layer is to test how the resolvability of tilted angle φ is between TTI and VTI media. Fig. 8d shows that the TTI parameters can be well resolved after ten iterations under an ideal situation with noise-free data, though the initial reference values differ much from the true model values. The details of each inverted parameter are shown in Table 4. The well-resolved δ is expected in this experiment because this geometry provides sufficient ray angles around 45°. Large offset in this setup provides wide ray angles and make estimating accurate ε become feasible. This experiment indicates that to reliably estimate ε and δ together, long offset and well control are necessary.

The above tests indicate that the seismic acquisition geometry plays a significant role on anisotropic parameter estimation. A practical workflow can be designed to progressively invert for anisotropic parameters and minimize the influence of errors in one parameter on estimating the other parameters based on the sensitivity analyses of analytical kernels. To quantify the effects of errors in the TTI parameters and facilitate designing this workflow, we repeated the TTI layered traveltime tomography to invert for ε and δ under different assumptions for axial velocity but using known layer geometry and tilted angle of symmetry axes. The errors in axial velocity are considered as noises in the data space. After the tenth iteration of tomography, we notice that even 5% errors in axial velocity will bring more than 10% errors for ε and more than 15% errors for δ. This experiment shows that axial velocity could play the most important role in estimating any other parameters. The larger errors on inverted δ model are because parameter δ is coupled with axial velocity which forms the moveout velocity. Any errors in axial velocity will bring large deviation on traveltime to underdetermine δ from traveltime data. The comparison between different kernels on varying ray angles (Fig. 3) shows that even at ray angle 45°, where the peak magnitude of kernel δ presents, the peak magnitude of axial velocity is still five to six times greater than δ. Either reason will make inverting for δ difficult. However, in VSP acquisition geometry, the velocity along well-bore are typically known and can be measured directly. This provides a good opportunity to estimate ε and δ together from layered traveltime tomography.

3.4. 3D layered model TTI parameter estimation using VSP first arrivals

In 3D TTI layered traveltime tomography there are two different assumptions on the tilted angle of the symmetry axis (Fig. 9). The first one assumes that each model layer has a constant orientation of the symmetry axis as described by its tilted angle φ and azimuth angle ψ. However, geological interpretations indicate that it is rare that the symmetry axes in 3D deformable plane are expressed by only two angles. Some previous studies took the second assumption that the tilted symmetry axis is perpendicular to the orientation of each layer (Grechka, 2009).

To examine the capability of the 3D TTI layered traveltime tomography, a synthetic true model is constructed with four TTI layers and each layer has different anisotropic parameters. The tilted symmetry axis is assumed to be perpendicular to bedding. Since tilted symmetry axes have been defined, in this test, we can use Eq. (4) to combine with isotropic shortest-path ray tracing algorithm (Moser,

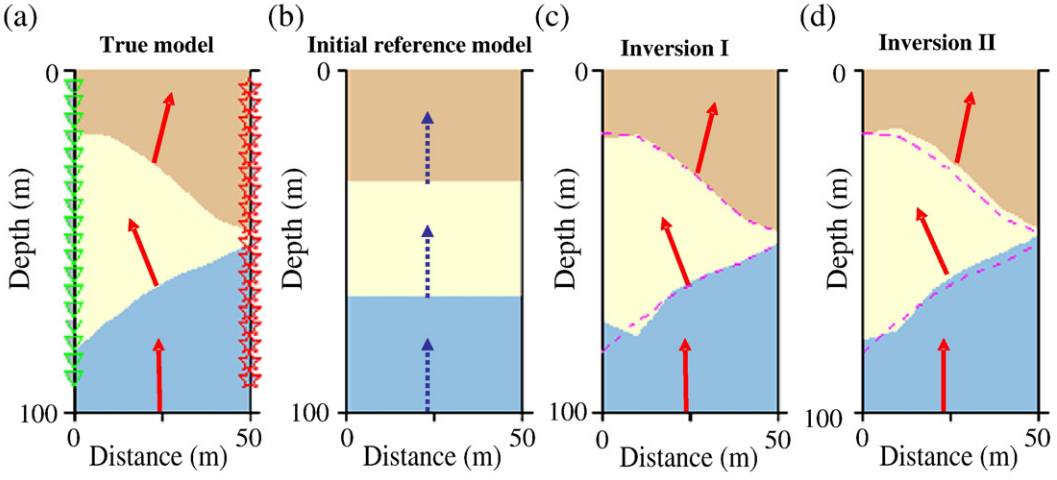

	True model			Inversion I		Inversion II	
	ε	ϕ	δ	ε	ϕ	ε	ϕ
Layer1	0.15	-14°	0.10	0.15	-14.079°	0.151	-12.559°
Layer2	0.10	22°	0.04	0.101	21.233°	0.095	26.584°
Layer3	0.14	1°	0.15	0.134	1.492°	0.156	-0.71°

Fig. 6. 2D TTI crosswell test. (a) True model; (b) reference model; (c) the result of inversion I with δ of 0.1, 0.04, 0.15 in each layer; and (d) the result of inversion II with δ of 0.0, 0.0, 0.0 in each layer. Red arrows represent true symmetry axes in (a) and inverted symmetry axes in (b) and (d). Blue arrows denote the initial vertical symmetry axes.

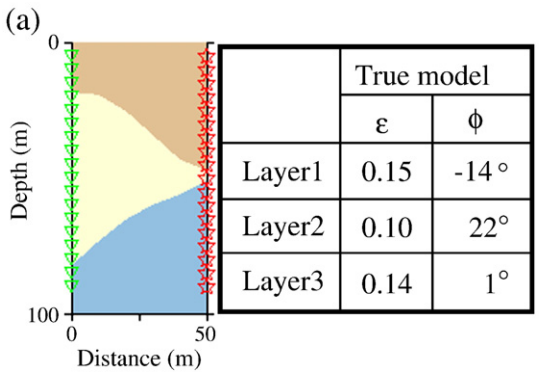

	True model	
	ε	ϕ
Layer1	0.15	-14°
Layer2	0.10	22°
Layer3	0.14	1°

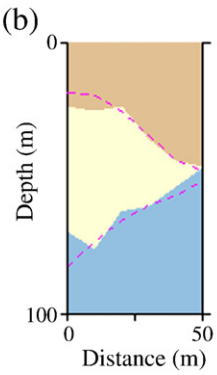

	Inversion result	
	ε	ϕ
Layer1	0.158	-17.27°
Layer2	0.103	27.82°
Layer3	0.124	-8.71°

Fig. 7. 2D Crosswell tomography by adding 5% Gaussian noise when inverting for layer geometry, ε and φ. (a) True model. (b) Inversion result. In this test, the inversion parameters are layer geometry, ε and tilted angle φ.

1991) in 3D anisotropic media to generate first arrivals. Fig. 10 shows raypaths from many surface sources to a receiver in the wellbore for both an isotropic model and a TTI model. Here, we invert for parameter ε and δ together. Table 5 shows the results of layered anisotropic estimation by inverting ε and δ after ten tomographic iterations. The large number of 1004 sources from different azimuth directions improves the ray coverage. The average inversion errors for both parameters are comparable, for ε is 0.5% and for δ is 0.61%. The minor differences between the true parameters and estimated parameters are expected and are caused primarily by deficiencies in the ray coverage along certain angles. Although this test shows the good capability to recover the layered parameters, any incomplete ray coverage will make it very difficult to recover all the anisotropic parameters. This experiment shows a familiar trend that in 2D cases, which illustrate that at large offset with well control, ε and δ can be estimated simultaneously by traveltime tomography.

According to the analyses of statistic errors, the practice strategy for the workflow of the TTI layered traveltime tomography can be proposed. Axial velocity and layer geometry (Jiang et al., 2009) should be always treated as priority parameters for velocity model building. For crosswell acquisition, ε could be estimated accurately and should be considered as priority parameters. For VSP acquisition geometry, δ should be estimated before ε (Fig. 11).

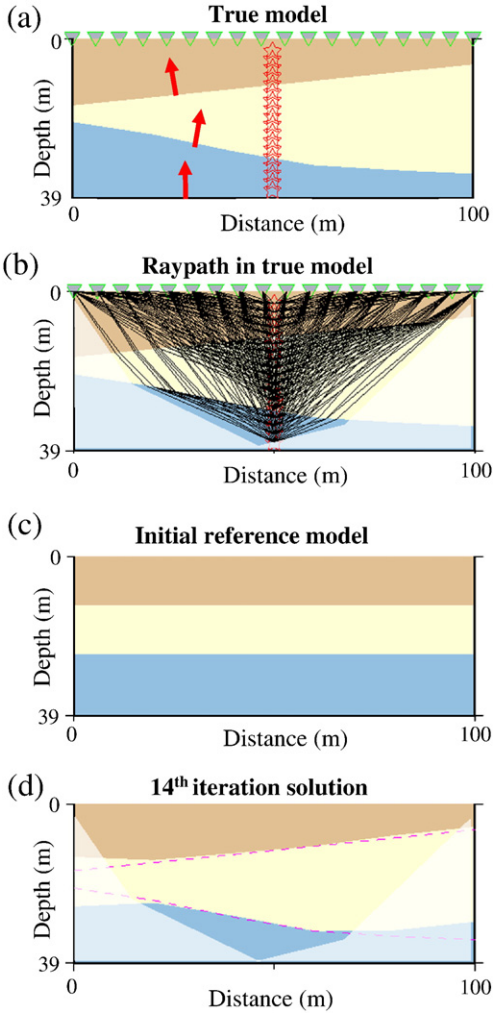

Fig. 8. 2D layered TTI tomography by VSP first arrivals. (a) True TTI model and the distributions of sources (triangles) and receivers (stars). The arrows denote the tilted angles of symmetry in the layer anisotropic velocities. (b) TTI ray tracing in true model. (c) Initial reference model with isotropic assumptions. (d) Inverted model. The dash lines indicate the true interface geometry. The axial velocities are fixed during the inversion process. In panels (b) and (d) the region outside ray coverage is lightened.

4. Discussion

Though good estimates of the anisotropic velocity structure will enhance the quality of depth imaging, the results from many anisotropic depth-imaging projects are disappointing because estimating anisotropic parameters in depth domain depends on many elements. Sparse and irregular data acquisition, incomplete illumination of subsurface strata and erroneous data with low signal-to-noise ratios may result in incorrect estimates, nonlinear relation between model and data space makes inversion underdetermined or overdetermined. In this study we intend to quantify the feasibility of the TTI layered traveltime tomography in estimating the anisotropic parameters in the thickness-varying layered models. The traveltime equation leads to analytical kernels for different anisotropic parameters that illuminate the sensitivity of each anisotropic parameter with respect to various types of noise in the traveltime data, including the noise due to errors in some of the model parameters. Our error analysis suggests a practice strategy to first invert for the most noise-tolerant model parameters axial velocity and ε in crosswell acquisition

Table 4
2D layered anisotropic parameter estimation using noise-free VSP first arrivals.

	True model		Initial reference model		Inverted model	
	ε	δ	ε	δ	ε	δ
Layer 1	0.15	0.10	0.0	0.0	0.150	0.100
Layer 2	0.10	0.04	0.0	0.0	0.093	0.038
Layer 3	0.14	0.15	0.0	0.0	0.134	0.135

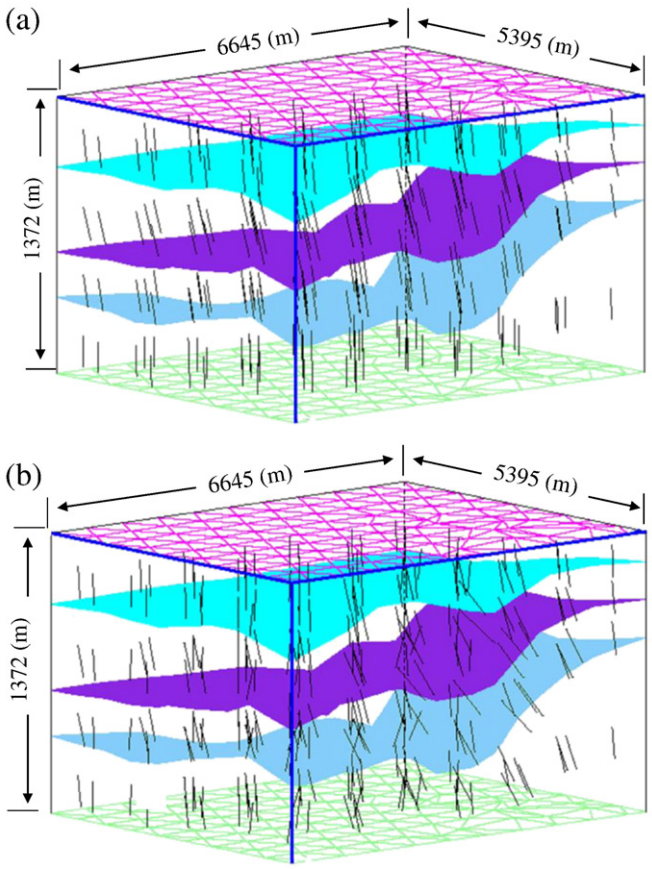

Fig. 9. Two assumptions of the tilted symmetry axis in 3D layered model. (a) Each layer has constant tilted angle φ and azimuth angle ψ of the symmetry axis. (b) The symmetry axis is perpendicular to the layer interface at each location.

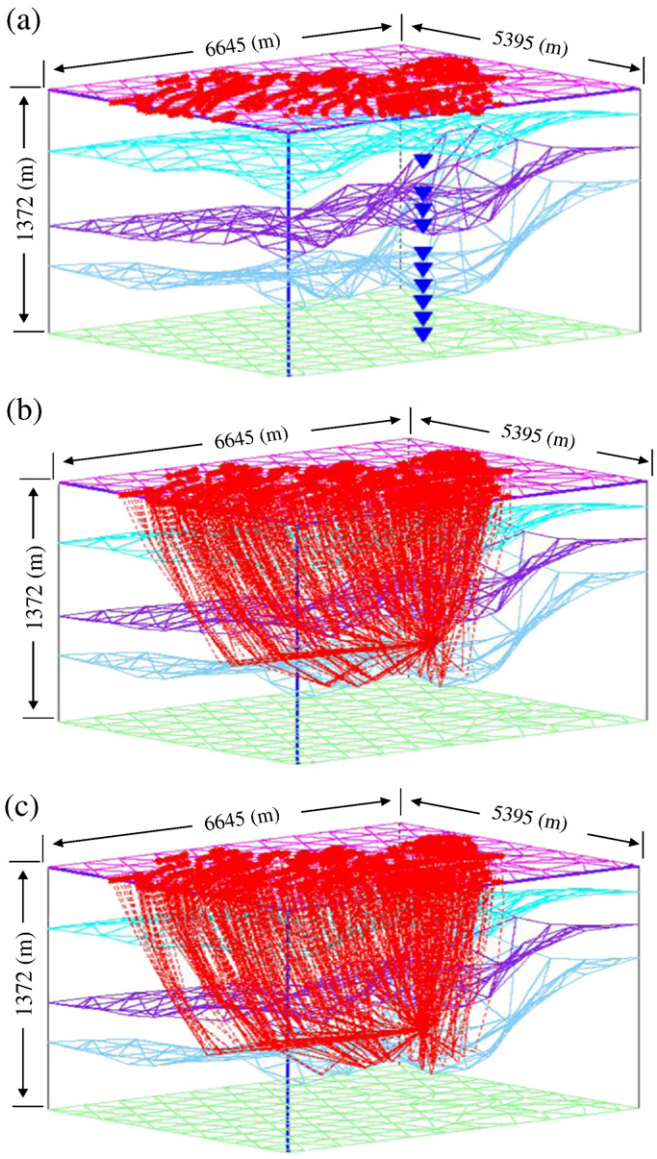

Fig. 10. 3D ray tracing in isotropic and TTI media. (a) Model geometry and distributions of surface sources (stars) and in-wellbore receivers (solid triangles). (b) Raypaths (dashed lines) in isotropic reference model from one receiver located in the third layer. (c) Raypaths in synthetic TTI model with the assumption of the tilted symmetry axis perpendicular to the layer interface.

geometry, and to progressively include the inversions for other parameters when the ray coverage is sufficient, however, in VSP acquisition geometry, the estimating of axial velocity and δ should be considered as a conventional workflow for velocity model building in anisotropic media.

In our model setup each anisotropic model layer has five types of parameters: the velocity along the symmetry axis, the thickness-varying interface, Thomsen's anisotropic parameters ε and δ, and the tilted angle φ of the symmetry axis. The quality of the model parameterization and the initial estimates of the model variables depend largely on the available geological and geophysical information. In the model parameterization process we shall always try to develop realistic but simple models that will help reduce the nonuniqueness in the model building process.

Our analysis indicates that inversions for the tilted symmetry axes of the TTI models create a new ambiguity in anisotropic tomography. The errors in the assumptions that the symmetry axis is vertical (VTI) or horizontal (HTI) may degrade the quality of the parameter estimation for the TTI media and lead to significant distortions in the image quality. To estimate anisotropic parameter, different acquisition offsets can provide different aspects (Li and Yuan, 1999). Generally, small offset is used for determining check-shot velocity, or axial velocity. Intermediate offset is good for determining moveout velocity, therefore parameter δ could be iteratively resolved. Because parameter δ is coupled with axial velocity, any errors from the measurement on axial velocity V_{p0} will result in instability for building δ model. Large offset is good for estimating parameter ε since most rays will travel horizontally. However, any gaps or deficiencies in the raypath coverage could affect the resolution of the tomographic results, and the most effective solution is to use wide-azimuth data with a wide spread of sources and receivers.

Although the synthetic tests in this paper show good probability to invert for several anisotropic parameters using first arrivals, field data may bring more challenges. For example, irregular acquisitions can limit the range of the ray coverage and result in deficiencies in the raypath directions, low signal to noise ratio will increase the difficulty

Table 5
3D layered anisotropic parameter estimation by inverting ε and δ together.

	True model		Reference model		Inverted model	
	ε	δ	ε	δ	ε	δ
Layer 1	0.12	0.03	0.0	0.0	0.119	0.029
Layer 2	0.14	0.05	0.0	0.0	0.140	0.057
Layer 3	0.16	0.07	0.0	0.0	0.163	0.065
Layer 4	0.18	0.09	0.0	0.0	0.180	0.091

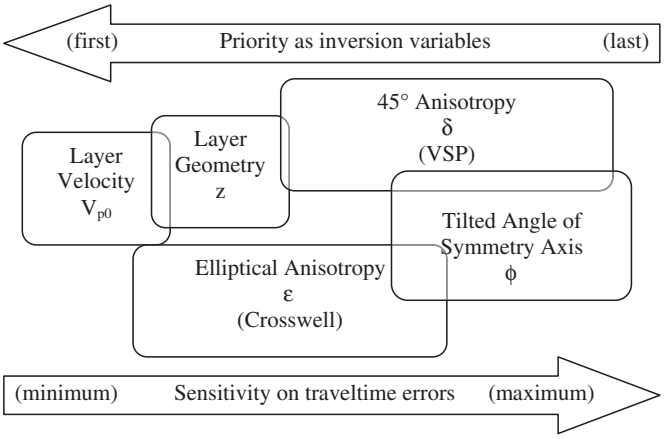

Fig. 11. A general workflow developed for layered anisotropic parameter estimation.

and errors in picking the first arrivals. Nevertheless, we expect the general trends of the relative resolvability of different anisotropic variables as revealed by our systematic evaluations of synthetic models will hold true. The choices on the complexity levels of the anisotropic depth model and what parameters to be inverted depend on the available data quality, coverage, and study objectives.

5. Conclusions

We devise a TTI layered traveltime tomography method to invert for anisotropic depth models with several thickness-varying layers using the first arrivals. By applying this tomography method to a series of synthetic depth velocity models of tilted transverse isotropy, we evaluate the relative influence of errors in some of the model parameters on the inversion results of other parameters. The influence of the errors in δ on the other model parameters is smaller than that of the reverse situation in crosswell acquisition geometry. In VSP acquisition geometry, layer velocity and δ are the most sensitive parameters with traveltime data. Our analysis suggests a practical strategy to take layer velocity and ε as priority inversion parameters in crosswell acquisition geometry, but the estimating of layer velocity and δ progressively in VSP acquisition geometry shall enhance the stability of anisotropic velocity model building.

References

Alkhalifah, T., 1997. Velocity analysis using nonhyperbolic moveout in transversely isotropic media. Geophysics 62, 1839–1854.
Alkhalifah, T., Tsvankin, I., 1995. Velocity analysis for transversely isotropic media. Geophysics 60, 1550–1566.
Ball, G., 1995. Estimation of anisotropy and anisotropic 3-D prestack depth migration, offshore Zaire. Geophysics 60, 1495–1513.
Berryman, J.G., Grechka, V.Y., Berge, P.A., 1999. Analysis of Thomsen parameters for finely layered VTI media. Geophysical Prospecting 47, 959–978.
Bishop, T.N., Bube, K.P., Cutler, R.T., Langan, R.T., Love, P.L., Resnick, R.T., Shuey, R.T., Spindler, D.A., Wyld, H.W., 1985. Tomographic determination of velocity and depth in laterally varying media. Geophysics 50, 903–923.
Cerveny, V., 2001. Seismic Ray Theory. Cambridge University Press.
Chapman, C., Pratt, R., 1992. Traveltime tomography in anisotropic media—I. Theory. Geophysical Journal International 109, 1–19.
Charles, S., Mitchell, D., Holt, R., Lin, J., John, M., 2008. Data-driven tomographic velocity analysis in tilted transversely isotropic media: a 3 D case history from the Canadian Foothills. Geophysics 73, VE261–VE268.
Dewangan, P., Tsvankin, I., 2006. Velocity-independent layer stripping of PP and PS reflection traveltimes. Geophysics 71, U59–U65.
Grechka, V., 2009. On the nonuniqueness of traveltime inversion in elliptically anisotropic media. Geophysics 74, WB137–WB145.
Hornby, B., Schwartz, L., John, H., 1994. Anisotropic effective-medium modeling of the elastic properties of shales. Geophysics 59, 1570–1583.
Jiang, F., Zhou, H., Zou, Z., Liu, H., 2009. 2D Tomographic velocity model building in tilted transversely isotropic media. 79th Annual International Meeting, SEG, Expanded Abstract, pp. 4024–4028.
Kosloff, D., Sherwood, J., Koren, Z., Machet, E., Falkovitz, Y., 1996. Velocity and interface depth determination by tomography of depth migrated gathers. Geophysics 61, 1511–1523.
Kumar, C., Sen, M.K., Ferguson, R.J., 2004. Traveltime calculation and prestack depth migration in tilted transversely isotropic media. Geophysics 69, 37–44.
Kumar, D., Sen, M.K., Ferguson, R.J., 2008. Depth migration anisotropy analysis in the time domain. Geophysical Prospecting 56, 87–94.
Li, X., Yuan, J., 1999. Converted-wave moveout and parameter estimation for transverse isotropy. 61st EAGE conference, Expanded Abstract I, p. 4035.
Maultzsch, S., Chapman, M., Liu, E., Li, X., 2007. Modeling and analysis of attenuation anisotropy in multi-azimuth VSP data from the Clair field. Geophysical Prospecting 627–642.
Moser, T.J., 1991. Shortest path calculation of seismic rays. Geophysics 56, 59–67.
Pratt, R.G., Shin, C., Hicks, G.J., 1998. Gauss–Newton and full Newton methods in frequency–space seismic waveform inversion. Geophysical Journal International 133, 341–362.
Sayers, C., 2005. Seismic anisotropy of shales. Geophysical Prospecting 53, 667–676.
Scales, J.A., 1987. Tomographic inversion via the conjugate gradient method. Geophysics 52, 179–185.
Sen, M.K., Mukherjee, A., 2003. τ-p analysis in transversely isotropic media. Geophysical Journal International 154, 647–658.
Sena, A., 1991. Seismic traveltime equations for azimuthally anisotropic and isotropic media: estimation of interval elastic properties. Geophysics 56, 2090–2101.
Slawinski, M.A., Lamoureux, M.P., Slawinski, R.A., Brown, R.J., 2003. VSP traveltime inversion for anisotropy in buried layer. Geophysical Prospecting 131–139.
Thomsen, L., 1986. Weak elastic anisotropy. Geophysics 51, 1954–1966.
Tsvankin, I., 2001. Seismic Signatures and Analysis of Reflection Data in Anisotropic Media. Elsevier Science Publ. Co., Inc.
Tsvankin, I., Thomsen, L., 1994. Non-hyperbolic reflection moveout in anisotropic media. Geophysics 59, 1290–1304.
Watanabe, T., Hirai, T., Sassa, K., 1996. Seismic traveltime tomography in anisotropic heterogeneous media. Journal of Applied Geophysics 35, 133–143.
Zhou, H., 2003. Multiscale traveltime tomography. Geophysics 68, 1639–1649.
Zhou, H., 2006. Multiscale deformable-layer tomography. Geophysics 71, R11–R19.
Zhou, B., Greenhalgh, S., 2009. On the computation of the Frechet derivatives for seismic waveform inversion in 3D general anisotropic, heterogeneous media. Geophysics 74, WB153–WB163.
Zhou, H., Zhang, G., Bloor, R., 2006. An anisotropic acoustic wave equation for VTI media. 68th Annual Conference and Exhibition, EAGE, Extended Abstracts, p. H033.
Zhou, B., Greenhalgh, S., Alan, G., 2008. Nonlinear traveltime inversion scheme for crosshole seismic tomography in tilted transversely isotropic media. Geophysics 73, D17–D33.